European Organisation for Nuclear Research

CERN-EP/2000-156
22 December, 2000

Search for the Standard Model Higgs Boson in e^+e^- Collisions at $\sqrt{s} \approx 192$–209 GeV

The OPAL Collaboration

Abstract

A search for the Standard Model Higgs boson has been performed with the OPAL detector at LEP based on the full data sample collected at $\sqrt{s} \approx 192$–209 GeV in 1999 and 2000, corresponding to an integrated luminosity of approximately 426 pb^{-1}. The data are examined for their consistency with the background-only hypothesis and various Higgs boson mass hypotheses. A lower bound of 109.7 GeV is obtained on the Higgs boson mass at the 95% confidence level. At higher masses, the data are consistent with both the background and the signal-plus-background hypotheses.

(Accepted by Physics Letters B)

This work is dedicated to the memory of our friends and collaborators, Professors Shuji Orito and George A. Snow.

The OPAL Collaboration

G. Abbiendi[2], C. Ainsley[5], P.F. Åkesson[3], G. Alexander[22], J. Allison[16], G. Anagnostou[1], K.J. Anderson[9], S. Arcelli[17], S. Asai[23], D. Axen[27], G. Azuelos[18,a], I. Bailey[26], A.H. Ball[8], E. Barberio[8], R.J. Barlow[16], R.J. Batley[5], T. Behnke[25], K.W. Bell[20], G. Bella[22], A. Bellerive[9], G. Benelli[2], S. Bethke[32], O. Biebel[32], I.J. Bloodworth[1], O. Boeriu[10], P. Bock[11], J. Böhme[25], D. Bonacorsi[2], M. Boutemeur[31], S. Braibant[8], P. Bright-Thomas[1], L. Brigliadori[2], R.M. Brown[20], H.J. Burckhart[8], J. Cammin[3], P. Capiluppi[2], R.K. Carnegie[6], B. Caron[28], A.A. Carter[13], J.R. Carter[5], C.Y. Chang[17], D.G. Charlton[1,b], P.E.L. Clarke[15], E. Clay[15], I. Cohen[22], J. Couchman[15], A. Csilling[15,i], M. Cuffiani[2], S. Dado[21], G.M. Dallavalle[2], S. Dallison[16], A. De Roeck[8], E.A. De Wolf[8], P. Dervan[15], K. Desch[25], B. Dienes[30,f], M.S. Dixit[7], M. Donkers[6], J. Dubbert[31], E. Duchovni[24], G. Duckeck[31], I.P. Duerdoth[16], P.G. Estabrooks[6], E. Etzion[22], F. Fabbri[2], M. Fanti[2], L. Feld[10], P. Ferrari[12], F. Fiedler[8], I. Fleck[10], M. Ford[5], A. Frey[8], A. Fürtjes[8], D.I. Futyan[16], P. Gagnon[12], J.W. Gary[4], G. Gaycken[25], C. Geich-Gimbel[3], G. Giacomelli[2], P. Giacomelli[8], D. Glenzinski[9], J. Goldberg[21], C. Grandi[2], K. Graham[26], E. Gross[24], J. Grunhaus[22], M. Gruwé[08], P.O. Günther[3], A. Gupta[9], C. Hajdu[29], G.G. Hanson[12], K. Harder[25], A. Harel[21], M. Harin-Dirac[4], M. Hauschild[8], C.M. Hawkes[1], R. Hawkings[8], R.J. Hemingway[6], C. Hensel[25], G. Herten[10], R.D. Heuer[25], J.C. Hill[5], K. Hoffman[8], R.J. Homer[1], A.K. Honma[8], D. Horváth[29,c], K.R. Hossain[28], R. Howard[27], P. Hüntemeyer[25], P. Igo-Kemenes[11], K. Ishii[23], A. Jawahery[17], H. Jeremie[18], C.R. Jones[5], P. Jovanovic[1], T.R. Junk[6], N. Kanaya[23], J. Kanzaki[23], G. Karapetian[18], D. Karlen[6], V. Kartvelishvili[16], K. Kawagoe[23], T. Kawamoto[23], R.K. Keeler[26], R.G. Kellogg[17], B.W. Kennedy[20], D.H. Kim[19], K. Klein[11], A. Klier[24], S. Kluth[32], T. Kobayashi[23], M. Kobel[3], T.P. Kokott[3], S. Komamiya[23], R.V. Kowalewski[26], T. Kämer[25], T. Kress[4], P. Krieger[6], J. von Krogh[11], D. Krop[12], T. Kuhl[3], M. Kupper[24], P. Kyberd[13], G.D. Lafferty[16], H. Landsman[21], D. Lanske[14], I. Lawson[26], J.G. Layter[4], A. Leins[31], D. Lellouch[24], J. Letts[12], L. Levinson[24], R. Liebisch[11], J. Lillich[10], C. Littlewood[5], A.W. Lloyd[1], S.L. Lloyd[13], F.K. Loebinger[16], G.D. Long[26], M.J. Losty[7], J. Lu[27], J. Ludwig[10], A. Macchiolo[18], A. Macpherson[28,l], W. Mader[3], S. Marcellini[2], T.E. Marchant[16], A.J. Martin[13], J.P. Martin[18], G. Martinez[17], T. Mashimo[23], P. Mättig[24], W.J. McDonald[28], J. McKenna[27], T.J. McMahon[1], R.A. McPherson[26], F. Meijers[8], P. Mendez-Lorenzo[31], W. Menges[25], F.S. Merritt[9], H. Mes[7], A. Michelini[2], S. Mihara[23], G. Mikenberg[24], D.J. Miller[15], W. Mohr[10], A. Montanari[2], T. Mori[23], K. Nagai[13], I. Nakamura[23], H.A. Neal[33], R. Nisius[8], S.W. O'Neale[1], F.G. Oakham[7], F. Odorici[2], A. Oh[8], A. Okpara[11], M.J. Oreglia[9], S. Orito[23], C. Pahl[32], G. Pásztor[8,i], J.R. Pater[16], G.N. Patrick[20], J.E. Pilcher[9], J. Pinfold[28], D.E. Plane[8], B. Poli[2], J. Polok[8], O. Pooth[8], A. Quadt[8], K. Rabbertz[8], C. Rembser[8], P. Renkel[24], H. Rick[4], N. Rodning[28], J.M. Roney[26], S. Rosati[3], K. Roscoe[16], A.M. Rossi[2], Y. Rozen[21], K. Runge[10], O. Runolfsson[8], D.R. Rust[12], K. Sachs[6], T. Saeki[23], O. Sahr[31], E.K.G. Sarkisyan[8,m], C. Sbarra[26], A.D. Schaile[31], O. Schaile[31], P. Scharff-Hansen[8], M. Schröder[8], M. Schumacher[25], C. Schwick[8], W.G. Scott[20], R. Seuster[14,g], T.G. Shears[8,j], B.C. Shen[4], C.H. Shepherd-Themistocleous[5], P. Sherwood[15], G.P. Siroli[2], A. Skuja[17], A.M. Smith[8], G.A. Snow[17], R. Sobie[26], S. Söldner-Rembold[10,e], S. Spagnolo[20], F. Spano[9], M. Sproston[20], A. Stahl[3], K. Stephens[16], D. Strom[19], R. Ströhmer[31], L. Stumpf[26], B. Surrow[8], S.D. Talbot[1], S. Tarem[21], M. Tasevsky[8], R.J. Taylor[15], R. Teuscher[9], J. Thomas[15], M.A. Thomson[5], E. Torrence[9], S. Towers[6], D. Toya[23], T. Trefzger[31], I. Trigger[8],

Z. Trócsányi[30,f], E. Tsur[22], M.F. Turner-Watson[1], I. Ueda[23], B. Vachon[26], C.F. Vollmer[31], P. Vannerem[10], M. Verzocchi[8], H. Voss[8], J. Vossebeld[8], D. Waller[6], C.P. Ward[5], D.R. Ward[5], P.M. Watkins[1], A.T. Watson[1], N.K. Watson[1], P.S. Wells[8], T. Wengler[8], N. Wermes[3], D. Wetterling[11] J.S. White[6], G.W. Wilson[16], J.A. Wilson[1], T.R. Wyatt[16], S. Yamashita[23], V. Zacek[18], D. Zer-Zion[8,k]

[1]School of Physics and Astronomy, University of Birmingham, Birmingham B15 2TT, UK
[2]Dipartimento di Fisica dell' Università di Bologna and INFN, I-40126 Bologna, Italy
[3]Physikalisches Institut, Universität Bonn, D-53115 Bonn, Germany
[4]Department of Physics, University of California, Riverside CA 92521, USA
[5]Cavendish Laboratory, Cambridge CB3 0HE, UK
[6]Ottawa-Carleton Institute for Physics, Department of Physics, Carleton University, Ottawa, Ontario K1S 5B6, Canada
[7]Centre for Research in Particle Physics, Carleton University, Ottawa, Ontario K1S 5B6, Canada
[8]CERN, European Organisation for Nuclear Research, CH-1211 Geneva 23, Switzerland
[9]Enrico Fermi Institute and Department of Physics, University of Chicago, Chicago IL 60637, USA
[10]Fakultät für Physik, Albert Ludwigs Universität, D-79104 Freiburg, Germany
[11]Physikalisches Institut, Universität Heidelberg, D-69120 Heidelberg, Germany
[12]Indiana University, Department of Physics, Swain Hall West 117, Bloomington IN 47405, USA
[13]Queen Mary and Westfield College, University of London, London E1 4NS, UK
[14]Technische Hochschule Aachen, III Physikalisches Institut, Sommerfeldstrasse 26-28, D-52056 Aachen, Germany
[15]University College London, London WC1E 6BT, UK
[16]Department of Physics, Schuster Laboratory, The University, Manchester M13 9PL, UK
[17]Department of Physics, University of Maryland, College Park, MD 20742, USA
[18]Laboratoire de Physique Nucléaire, Université de Montréal, Montréal, Quebec H3C 3J7, Canada
[19]University of Oregon, Department of Physics, Eugene OR 97403, USA
[20]CLRC Rutherford Appleton Laboratory, Chilton, Didcot, Oxfordshire OX11 0QX, UK
[21]Department of Physics, Technion-Israel Institute of Technology, Haifa 32000, Israel
[22]Department of Physics and Astronomy, Tel Aviv University, Tel Aviv 69978, Israel
[23]International Centre for Elementary Particle Physics and Department of Physics, University of Tokyo, Tokyo 113-0033, and Kobe University, Kobe 657-8501, Japan
[24]Particle Physics Department, Weizmann Institute of Science, Rehovot 76100, Israel
[25]Universität Hamburg/DESY, II Institut für Experimental Physik, Notkestrasse 85, D-22607 Hamburg, Germany
[26]University of Victoria, Department of Physics, P O Box 3055, Victoria BC V8W 3P6, Canada
[27]University of British Columbia, Department of Physics, Vancouver BC V6T 1Z1, Canada
[28]University of Alberta, Department of Physics, Edmonton AB T6G 2J1, Canada
[29]Research Institute for Particle and Nuclear Physics, H-1525 Budapest, P O Box 49, Hungary
[30]Institute of Nuclear Research, H-4001 Debrecen, P O Box 51, Hungary

[31]Ludwigs-Maximilians-Universität München, Sektion Physik, Am Coulombwall 1, D-85748 Garching, Germany
[32]Max-Planck-Institute für Physik, Föhring Ring 6, 80805 München, Germany
[33]Yale University,Department of Physics,New Haven, CT 06520, USA

[a] and at TRIUMF, Vancouver, Canada V6T 2A3
[b] and Royal Society University Research Fellow
[c] and Institute of Nuclear Research, Debrecen, Hungary
[e] and Heisenberg Fellow
[f] and Department of Experimental Physics, Lajos Kossuth University, Debrecen, Hungary
[g] and MPI München
[i] and Research Institute for Particle and Nuclear Physics, Budapest, Hungary
[j] now at University of Liverpool, Dept of Physics, Liverpool L69 3BX, UK
[k] and University of California, Riverside, High Energy Physics Group, CA 92521, USA
[l] and CERN, EP Div, 1211 Geneva 23
[m] and Tel Aviv University, School of Physics and Astronomy, Tel Aviv 69978, Israel.

1 Introduction

In the Standard Model [1], the Higgs mechanism [2] gives mass to the electroweak gauge bosons, thus allowing the unification of the electromagnetic and weak interactions. Whether the Higgs boson exists is one of the most important open questions in particle physics. A number of improvements were made to the LEP collider for the year 2000 data taking, which increased the Higgs discovery potential, extending the sensitivity of the Higgs boson search to approximately 115 GeV if the data from all four LEP experiments are combined. The combination of the preliminary Higgs boson search results of the four LEP experiments [3, 4] shows an excess of candidates which may indicate the production of a Standard Model Higgs boson with a mass near 115 GeV. In this letter we present the results of a search for the Standard Model Higgs boson with the OPAL detector at LEP, considering particularly the mass hypothesis of 115 GeV.

Approximately 426 pb^{-1} of $\mathrm{e}^+\mathrm{e}^-$ annihilation data were collected by OPAL in the years 1999 and 2000 at centre-of-mass energies in the range 192–209 GeV; this data sample is used for the analyses presented in this letter. Searches are performed for the "Higgs-strahlung" process $\mathrm{e}^+\mathrm{e}^-\to\mathrm{H}^0\mathrm{Z}^0\to\mathrm{H}^0\mathrm{f}\bar{\mathrm{f}}$, where H^0 is the Standard Model Higgs boson, and $\mathrm{f}\bar{\mathrm{f}}$ is a fermion-antifermion pair from the Z^0 decay. For the $\mathrm{H}^0\nu\bar{\nu}$ ($\mathrm{H}^0\mathrm{e}^+\mathrm{e}^-$) final state, the contribution from the $\mathrm{W}^+\mathrm{W}^-$ ($\mathrm{Z}^0\mathrm{Z}^0$) fusion process is also taken into account. Only the decays of the Higgs boson into $\mathrm{b}\bar{\mathrm{b}}$ and $\tau^+\tau^-$ are considered here. OPAL has already reported results from the Standard Model Higgs boson search at $\mathrm{e}^+\mathrm{e}^-$ centre-of-mass energies up to 189 GeV [5, 6], where a lower mass limit of $m_{\mathrm{H}} > 91.0$ GeV was obtained at the 95% confidence level. A similar search procedure is applied here. All data were processed with the most up-to-date detector calibrations available. For future publications more refined analyses and the final detector calibrations will be used.

2 OPAL Detector, Data and Monte Carlo Samples

Details of the OPAL detector can be found in [7]. The data used in the analyses correspond to integrated luminosities of approximately 216 pb^{-1} at 192–202 GeV, 80 pb^{-1} at 203–206 GeV, and 130 pb^{-1} at centre-of-mass energies higher than 206 GeV. The total luminosity used to search for the Higgs boson varies by $\pm 2\%$ from channel to channel, due to slightly different requirements on the operational status of different detector elements. During 2000 (1999), data were taken at $\sqrt{s}$ = 200-209 GeV (192-202 GeV) with a luminosity-weighted mean centre-of-mass energy of 206.1 (197.6) GeV.

A variety of Monte Carlo samples was generated at centre-of-mass energies between 192 and 210 GeV. Higgs boson production is modelled with the HZHA3 generator [8] for a wide range of Higgs boson masses. The size of these samples varies from 2000 to 10000 events for each mass and at each centre-of-mass energy. The background processes are simulated with typically more than 50 times the statistics of the corresponding data sample. The process $(\mathrm{Z}/\gamma)^*\to\mathrm{q}\bar{\mathrm{q}}(\gamma)$ is modelled with the KK2f generator using CEEX [9] for the modelling of the initial state radiation. The four-fermion processes (4f) are simulated using grc4f [10]. The two-photon and other two-fermion processes have a negligible impact on the results. The hadronisation process is simulated with JETSET/PYTHIA [11] with parameters described in [12]. In each search channel, the estimates of the signal efficiency and the selected background rate depend strongly on the centre-of-mass energy and are

thus interpolated on a fine grid. For each Monte Carlo sample, the full detector response is simulated in detail as described in [13].

3 Analysis Procedures

We search for Higgs production in the following final states: $H^0Z^0 \to b\bar{b}q\bar{q}$ (four-jet channel), $H^0Z^0 \to b\bar{b}\nu\bar{\nu}$ (missing-energy channel), $H^0Z^0 \to b\bar{b}\tau^+\tau^-$ and $\tau^+\tau^-q\bar{q}$ (tau channels), $H^0Z^0 \to b\bar{b}e^+e^-$ and $b\bar{b}\mu^+\mu^-$ (electron and muon channels). In each channel, a preselection is applied to ensure that the events are well measured and are consistent with the desired signal topology. A likelihood selection combining 6 to 10 variables depending on the search channel is then used to further enrich the signal.

We use the same analysis techniques described in a previous publication [5], namely event reconstruction, b-flavour tagging, lepton (electron, muon and tau) identification and kinematic fits to reconstruct the Higgs boson mass. The b-tagging variable $\mathcal{B}$ is evaluated for each jet to distinguish jets containing b-hadrons from those that do not. The tracking and b-tagging performance in the Monte Carlo simulation are tuned using 8.2 pb^{-1} of calibration data collected at $\sqrt{s} \approx m_Z$ at intervals during 1999 and 2000 with the same detector configuration and operating conditions as the high-energy data. Figure 1(a) shows the distribution of $\mathcal{B}$ for the calibration data. Comparisons between the data and the Monte Carlo simulation are shown in Figure 1(b) for jets which are found opposite to jets passing or failing the b-tagging requirement. The tagging efficiency for b-flavoured (udsc-flavoured) jets is modelled by the Monte Carlo simulation to within an accuracy of 2% (5%).

The performance of the b-tagging for the data taken at $\sqrt{s} \geq 192$ GeV is checked with samples of $q\bar{q}(\gamma)$ events by selecting hadronic events with the mass of the $q\bar{q}$ system near m_Z. Figure 1(c) shows the b-tagging variable $\mathcal{B}$ for jets opposite b-tagged jets in the 2000 sample. The efficiency for tagging udsc flavours is also checked by computing $\mathcal{B}$ for the jets in a sample of $W^+W^- \to q\overline{q}\ell\overline{\nu}$ (ℓ=e or μ) obtained with the selection used to measure the W^+W^- cross-section [14] as shown in Figure 1(d). The expectation from the Standard Model Monte Carlo describes the data within the relative statistical uncertainty of 5–10%. The results of these cross-checks are not used in the evaluation of the systematic uncertainties described below.

Sources of systematic uncertainties are investigated for their effect on the signal detection efficiencies and the Standard Model backgrounds. The error from the modelling of the likelihood selection input variables on the background (signal) rates is 4–8% (1–4%), depending on the channel. These uncertainties are evaluated based on comparisons of the distributions of the variables in the data and the Monte Carlo. Comparisons of alternative Monte Carlo generators for the backgrounds [9–11, 15] account for an additional 3–11% uncertainty in the background rates. The uncertainty in the four-fermion cross-section is taken to be ±2% [16]. The uncertainties on the detector performance, such as the spatial resolution of the tracking and the modelling of the efficiency of the silicon microvertex detector, are evaluated source by source with Monte Carlo studies. Recent improvements in the knowledge of heavy quark production processes and decays, such as the b-hadron charged decay multiplicity [17] and the gluon splitting rate to heavy quarks [18], are taken into account in the analyses by reweighting Monte Carlo events. The modelling of the b-hadron production and decay processes is constrained by various measurements summarized in [17]; residual uncertainties in these measurements result in

systematic uncertainties here. In particular, the b-hadron charged decay multiplicity n_B is varied within $n_B = 4.955 \pm 0.062$. The uncertainties from the fragmentation functions for b- and c-quarks are obtained by adjusting the mean energy $\langle x_E \rangle$ within the range allowed by the measurements. The charm and bottom-flavoured hadron lifetimes are varied within their errors with negligible effect on all search channels. The total uncertainties on the background (signal) rates are 11–15% (5–6%) varying from channel to channel.

3.1 Event Selections and Mass Reconstruction

The preselection requirements in the four-jet channel are identical to those of [5]. After the preselection, a likelihood selection based on eight variables is applied. For each selected candidate, two of the jets are associated to the H^0 using a likelihood method based on the kinematic fit result and the b-tagging information. The mass determined by a $\mathrm{H}^0\mathrm{Z}^0$ 5C kinematic fit for the chosen jet pair gives the reconstructed mass of the Higgs boson candidate, $m_{\mathrm{H}}^{\mathrm{rec}}$. Because of the constraints of the kinematic fit, $m_{\mathrm{H}}^{\mathrm{rec}} < \sqrt{s} - m_{\mathrm{Z}}$. The variables used in the likelihood selection for the 1999 data are the same as those used in our earlier analysis [5]. For the 2000 data, however, one variable, the χ^2 probability of the $\mathrm{H}^0\mathrm{Z}^0$ 5C kinematic fit, is replaced by the χ^2 probability of a fit imposing an equal-mass constraint as used in the OPAL W mass measurement [19] in order to further suppress the $\mathrm{Z}^0\mathrm{Z}^0$ background.

The selection of the missing-energy channel is very similar to [5]. The notable changes are: 1) tightening the requirement on the maximum fraction of the visible energy in the angular region $|\cos\theta| > 0.90$ from 50% to 20% in order to further suppress $\mathrm{q\bar{q}}(\gamma)$ background (changed only in the 2000 analysis); 2) a looser requirement on the missing mass which is now selected in the range from 40 to 140 GeV. Other small changes correspond to the scaling of cut values with $\sqrt{s}$ for variables related to the visible momenta. In the construction of the likelihood selection, two new variables are included: 1) the thrust value of the event, and 2) the angle between the missing momentum and the direction of the most energetic jet. This last variable adds discrimination power especially against the process $\mathrm{W}^+\mathrm{W}^- \to \mathrm{q\overline{q}}\ell\overline{\nu}$ in which the charged lepton is close to one of the jet axes. The reconstructed Higgs boson mass $m_{\mathrm{H}}^{\mathrm{rec}}$ is evaluated using a kinematic fit constraining the missing mass to the Z^0 mass. Because of the fit constraints, $m_{\mathrm{H}}^{\mathrm{rec}} < \sqrt{s} - m_{\mathrm{Z}}$.

The event selections in the tau, electron and muon channels are identical to the ones used in [5]. For the tau channel the reconstructed Higgs boson mass is evaluated (see [5]) with the 3C kinematic fit with the largest χ^2 probability fixing either the tau pair invariant mass or the jet pair invariant mass to the Z^0 mass. The reconstructed Higgs boson mass is determined by the recoil mass of the electron pair in the electron channel, and with the results of a 4C kinematic fit constraining energy and momentum in the muon channel. There is no upper bound of $m_{\mathrm{H}}^{\mathrm{rec}}$ at $\sqrt{s} - m_{\mathrm{Z}}$ in the electron and muon channels.

The numbers of events selected in each analysis after preselection and after the final likelihood selection are shown in Table 1 for the data taken at $\sqrt{s} \approx 192 - 209$ GeV. The errors on the background and signal expectations are the sums in quadrature of the individual systematic uncertainties. Distributions of the selection likelihood values $\mathcal{L}^{\mathrm{H}^0\mathrm{Z}^0}$ in all channels are shown in Figure 2. The number of selected events in all search channels is 156 with 146.1±11.9 expected from Standard Model background processes.

The distributions of the reconstructed masses of the selected events are shown in Figure 3. Note that all data taken in the wide $\sqrt{s}$ range from 192 to 209 GeV are summed in the figure, while the expected signal rates strongly depend on $\sqrt{s}$. The method used to

optimise the sensitivity to the signal is described in Section 3.2. The background accumulation at high reconstructed mass in the four-jet channel is dominated by $q\bar{q}$ events and jet-pairing combinatorial backgrounds from the Z^0Z^0 process. The $q\bar{q}$ background in the missing-energy channel also clusters at high reconstructed mass because $q\bar{q}$ events passing the selection requirements are largely composed of events with two or more undetected, energetic initial state radiation photons with a small momentum sum along the beam direction. The jets in such events are nearly back-to-back, which results in values of $m_{\mathrm{H}}^{\mathrm{rec}}$ near the maximum kinematically allowed in the fits, $\sqrt{s} - m_{\mathrm{Z}}$.

3.2 Confidence Level Calculations

After the event selections, all results from the various search channels are combined to test for the presence of a Standard Model Higgs boson signal. Previous data taken at centre-of-mass energies near or below 189 GeV have a negligible impact on the sensitivity to Higgs boson signals with $m_{\mathrm{H}} > 100$ GeV and are not included. The cross-sections used in computing the confidence level (CL) include the effects of W^+W^- and Z^0Z^0 fusion processes and their interference with the H^0Z^0 process in the missing-energy and electron channels respectively, as calculated using HZHA3 [8].

In order to compute the confidence levels, a test statistic is defined which expresses how signal-like the data are. The confidence levels are computed from the test statistic of the observed data and the expected distributions of the test statistic in a large number of simulated experiments under two hypotheses: the background-only hypothesis and the signal+background hypothesis. The test statistic chosen is the likelihood ratio Q, the ratio of the probability of observing the data given the signal+background hypothesis to the probability of observing the data given the background-only hypothesis [20, 21]. The results of all search channels are expressed in fine bins of discriminating variables, such as $m_{\mathrm{H}}^{\mathrm{rec}}$. The expected signal strength depends strongly on $\sqrt{s}$, hence the results are considered separately in fine divisions of $\sqrt{s}$. In each bin of each channel at each $\sqrt{s}$ the expected Higgs boson signal, s_i, and the Standard Model background rate, b_i, are estimated, and the observed data counts, n_i, are reported. The s_i depend on the mass of the Higgs boson under study (the "test mass"). Each bin is considered to be a statistically independent search obeying Poisson statistics. The likelihood ratio Q can then be computed [21] as $\ln Q = -\sum_i s_i + \sum_i n_i \ln(1 + s_i/b_i)$. Each event has a weight in the sum which depends on the signal-to-background ratio in the bin in which it is found; events may be classified by their local s/b values. The confidence level for the background hypothesis is $(1 - \mathrm{CL}_b)$ [21] which is the probability in an ensemble of background-only experiments of observing a more signal-like Q than is actually observed: $1 - \mathrm{CL}_b = P(Q > Q_{\mathrm{obs}}|\mathrm{background})$. A low value of $(1 - \mathrm{CL}_b)$ indicates an excess of candidates in data compared to the expectation from background. The distribution of $(1 - \mathrm{CL}_b)$ is uniform between 0 and 1 in an ensemble of background-only experiments.

Similarly, the confidence level for the signal+background hypothesis is $\mathrm{CL}_{s+b} = P(Q \leq Q_{\mathrm{obs}}|\mathrm{signal} + \mathrm{background})$, and is used to exclude the signal+background hypothesis if it has a small value. To eliminate the possibility of excluding a signal to which there is no sensitivity, a third quantity is defined $\mathrm{CL}_s = \mathrm{CL}_{s+b}/\mathrm{CL}_b$ [21]. Results are also presented in terms of the signal rate limit $n_{95} = g_{\mathrm{min}} \sum_i s_i$, where g_{min} is the smallest number such that the signal hypothesis consisting of $g_{\mathrm{min}} s_i$ in each bin yields $\mathrm{CL}_s = 0.05$. The signal rate limit n_{95} depends on the test mass. The technique used to perform the computation of the confidence levels is the same as is used in [6].

In our previous papers, the only discriminating variables used were the values of $m_{\mathrm{H}}^{\mathrm{rec}}$. Here, the discriminating power is improved by combining $m_{\mathrm{H}}^{\mathrm{rec}}$ with other variables. In the four-jet channel, after the jet pairing assignment and mass determination, a new test-mass-dependent variable $\mathcal{D}_{mass}$ is formed using a likelihood technique in order to investigate the compatibility with the signal production hypothesis for a Higgs boson of a specific test mass. The variable $\mathcal{D}_{mass}$ is based on the following four quantities: 1) the combined b-tagging variable $\mathcal{B}_{2jet}^{H}$ defined by $\mathcal{B}_{2jet}^{H} \equiv \mathcal{B}_1 \cdot \mathcal{B}_2/(\mathcal{B}_1 \cdot \mathcal{B}_2 + (1-\mathcal{B}_1)\cdot(1-\mathcal{B}_2))$ for the two jets with the most significant b tags; 2) the energy difference between the most energetic and the least energetic jets in the event; 3) β_{min}, a selection likelihood variable (see [6]); and 4) the reconstructed Higgs boson mass $m_{\mathrm{H}}^{\mathrm{rec}}$. Signal Monte Carlo samples were generated with Higgs boson masses in 1 GeV steps, and $\mathcal{D}_{mass}$ is interpolated between neighbouring test masses. The distribution of $\mathcal{D}_{mass}$ is shown for a test mass of 115 GeV in Figure 4(a).

In the missing-energy, electron and muon channels, the selection likelihood value, $\mathcal{L}^{\mathrm{H^0Z^0}}$, is used to form a two-dimensional discriminant ($\mathcal{L}^{\mathrm{H^0Z^0}}$, $m_{\mathrm{H}}^{\mathrm{rec}}$). The cut on $\mathcal{L}^{\mathrm{H^0Z^0}}$ is chosen to optimise the sensitivity of this new discriminant. In Figures 4(b) and (c), the reconstructed mass distributions are shown in slices of the selection likelihoods for the electron and muon channels, and for the missing-energy channel, respectively. In each channel, the enrichment of the signal depends on both the likelihood value and on $m_{\mathrm{H}}^{\mathrm{rec}}$. For the tau channels, only the reconstructed mass is used for the discriminant as in [5].

The systematic uncertainties on the signal and background expectations in each channel are treated using an extension of the method described in [22]. Uncertainties described in Section 3 are assumed to be 100% correlated if they arise from the same source in different channels, in the signal and background estimations, and at different centre-of-mass energies. The current uncertainty on the beam energy for the 2000 data is expected to be of the order of 100 MeV, and would therefore affect the limits by $\sim$ 200 MeV. The uncertainty on the integrated luminosity is estimated to be 0.3%. Both of these errors are neglected.

4 Results

Figure 5(a) shows $(1-\mathrm{CL}_b)$ as a function of the test mass m_{H}. It attains its lowest value of 0.02 at $m_{\mathrm{H}} = 107$ GeV, indicating a local excess of candidates. The probability to observe such an excess anywhere in the range of test masses between 100 and 120 GeV is approximately 10%, estimated from the size of the range and the reconstructed mass resolution. The value of $(1-\mathrm{CL}_b)$ observed at m_{H}=115 GeV is 0.2. Figure 5(a) also shows the expected $(1-\mathrm{CL}_b)$ in the presence of a 115 GeV Higgs boson signal.

The signal rate limit n_{95} is shown as a function of m_{H} in Figure 5 (b) together with its median expectation in an ensemble of background-only experiments. Figure 5 (b) also shows the expected accepted signal rate. Where the signal rate curve crosses the n_{95} curve is the 95% CL exclusion limit on m_{H}, and the expected limit is where the median expected n_{95} curve crosses the accepted signal rate curve. A lower mass bound of 109.7 GeV is obtained, and the expected limit is 112.5 GeV. In particular, the hypothesis m_{H}=107 GeV is excluded at the 98% CL ($\mathrm{CL}_s = 0.02$) even in the presence of the excess candidates because the excess in the data is not large enough to be consistent with the expected signal rate from a Standard Model Higgs boson of that mass.

The candidates with the largest weights, $\ln(1+s/b)$, in each channel for test masses

of 115 GeV are listed in Table 2. Figure 6 shows the distributions of $\ln(1 + s/b)$ of each candidate as a function of the Higgs boson test mass for the candidates collected in 1999 and 2000. The region of test mass for which a candidate's contribution is significant depends on the mass resolution of the candidates in the channel, and the normalization of the curve depends on the candidate b-tags, the kinematic variables, the Higgs boson cross-section and the local background near the reconstructed candidate mass. Deviations from smoothness of the curves are due to Monte Carlo statistics; this uncertainty is included in the confidence level computation.

The most significant candidate for a Higgs boson search for a test mass $m_{\mathrm{H}} = 115$ GeV (candidate #1) is found in the four-jet channel. For the jet-pairing chosen by the jet-pairing likelihood function, the event has a reconstructed Higgs boson mass of 110.7 GeV. The second most significant candidate (#2) is also found in the four-jet channel, with a reconstructed mass of 112.6 GeV. No jet pairing yields a reconstructed Higgs boson mass close to the Z^0 mass in either of these two candidates.

The observed low value of $(1 - \mathrm{CL}_b)$ at 107 GeV is caused by candidates which have relatively high weights at around 105–110 GeV seen in Figure 6. For the tau channel candidate #5, the reconstructed mass is taken from the invariant mass of the jets after a 3C kinematic fit where the tau pair mass is constrained to the Z^0 mass. The tau pair mass is 91 GeV if a 2C fit [5] is performed. The muon channel candidate #7 significantly affects the results of the confidence level calculations around 100–105 GeV since its likelihood $\mathcal{L}^{\mathrm{H}^0\mathrm{Z}^0}$ is very close to one.

The observed $-2\ln Q$ is shown as a function of the test mass m_{H} in Figure 7 (a). Also shown are the 68% and 95% probability contours centred on the median expectation. Figure 7 (b) shows the probability density functions of $-2\ln Q$ for the signal+background hypothesis with $m_{\mathrm{H}} = 115$ GeV, and also for the background hypothesis. The separation between the two hypotheses is not strong. The background confidence level $(1-\mathrm{CL}_b)$=0.2 is the integral of the background-only probability density to the left of the data observation, and $\mathrm{CL}_{s+b} = 0.4$ is the integral to the right of the data observation of the signal+background curve. The data are slightly more consistent with the presence of a 115 GeV Higgs boson than with the background alone.

5 Conclusions

A search for the Standard Model Higgs boson has been performed with the OPAL detector at LEP based on the full data sample collected at $\sqrt{s} \approx$192–209 GeV in 1999 and 2000. The largest deviation with respect to the expected Standard Model background in the confidence level for the background hypothesis, $(1 - \mathrm{CL}_b)$, is observed for a Higgs boson mass of 107 GeV with a minimum $(1 - \mathrm{CL}_b)$ of 0.02, but the observed excess is less significant than is expected for a Standard Model Higgs boson with a 107 GeV mass. A lower bound of 109.7 GeV on the mass of the Standard Model Higgs boson is obtained at the 95% confidence level while the median expectation for the background-only hypothesis is 112.5 GeV. For a Higgs boson with a mass of 115 GeV, $(1 - \mathrm{CL}_b)$ is approximately 0.2 while CL_{s+b} is approximately 0.4, indicating that the data slightly favour the hypothesis that a signal is present, but also that the data are consistent with the background hypothesis. These data alone provide little discrimination between the signal+background and background hypotheses for Higgs boson masses above 112 GeV, but more statistically

powerful conclusions may be reached by combining the data presented here with those of the other LEP experiments [23].

Acknowledgements

We particularly wish to thank the SL Division for the efficient operation of the LEP accelerator at all energies and for their continuing close cooperation with our experimental group. We thank our colleagues from CEA, DAPNIA/SPP, CE-Saclay for their efforts over the years on the time-of-flight and trigger systems which we continue to use. In addition to the support staff at our own institutions we are pleased to acknowledge the
Department of Energy, USA,
National Science Foundation, USA,
Particle Physics and Astronomy Research Council, UK,
Natural Sciences and Engineering Research Council, Canada,
Israel Science Foundation, administered by the Israel Academy of Science and Humanities,
Minerva Gesellschaft,
Benoziyo Center for High Energy Physics,
Japanese Ministry of Education, Science and Culture (the Monbusho) and a grant under the Monbusho International Science Research Program,
Japanese Society for the Promotion of Science (JSPS),
German Israeli Bi-national Science Foundation (GIF),
Bundesministerium für Bildung und Forschung, Germany,
National Research Council of Canada,
Research Corporation, USA,
Hungarian Foundation for Scientific Research, OTKA T-029328, T023793 and OTKA F-023259.

References

[1] S. Glashow, Nucl. Phys. **22** (1961) 579;
S. Weinberg, Phys. Rev. Lett. **19** (1967) 1264;
A. Salam, ed. N. Svartholm, *Elementary Particle Theory*, Almquist and Wiksells, Stockholm (1968) 367.

[2] P.W. Higgs, Phys. Lett. **12** (1964) 132;
F. Englert and R. Brout, Phys. Rev. Lett. **13** (1964) 321;
G.S. Guralnik, C.R. Hagen, and T.W.B. Kibble, Phys. Rev. Lett. **13** (1964) 585.

[3] P. Igo-Kemenes, presentation given to the LEP Experiments Committee open session, `http://lephiggs.web.cern.ch/LEPHIGGS/talks/index.html`, 3 November 2000.

[4] ALEPH Collaboration, R. Barate *et al.*, Phys. Lett. **B495** (2000) 1;
L3 Collaboration, M. Acciarri *et al.*, Phys. Lett. **B495** (2000) 18.

[5] OPAL Collaboration, G. Abbiendi *et al.*, Eur. Phys. J. **C12** (2000) 567.

[6] OPAL Collaboration, G. Abbiendi *et al.*, Eur. Phys. J. **C7** (1999) 407;
OPAL Collaboration, K. Ackerstaff *et al.*, Eur. Phys. J. **C1** (1998) 425.

[7] OPAL Collaboration, K. Ahmet *et al.*, Nucl. Instr. and Meth. **A305** (1991) 275;
S. Anderson *et al.*, Nucl. Instr. and Meth. A403 (1998) 326;
B.E. Anderson *et al.*, IEEE Trans. on Nucl. Science 41 (1994) 845;
G. Aguillion *et al.*, Nucl. Instr. and Meth. A417 (1998) 266.

[8] P. Janot *et al.*, in *Physics at LEP2,* edited by G. Altarelli, T. Sjöstrand and F. Zwirner, CERN 96-01 Vol. 2, 309.
For HZHA3 and HZHA2, see *http://alephwww.cern.ch/∼janot/Generators.html.*

[9] S. Jadach, B.F. Ward and Z. Was, Phys. Lett. **B449** (1999) 97.

[10] J. Fujimoto *et al.*, Comp. Phys. Comm. **100** (1997) 128;
Physics at LEP2, J. Fujimoto *et al.*, CERN 96-01, Vol. 2, 30.

[11] T. Sjöstrand, Comp. Phys. Comm. **82** (1994) 74;
T. Sjöstrand *et al.*, *High-Energy-Physics Event Generation with PYTHIA 6.1*, hep-ph/0010017 (2000), to be published in Comp. Phys. Comm.

[12] OPAL Collaboration, G. Alexander *et al.*, Z. Phys **C69** (1996) 543.

[13] J. Allison *et al.*, Nucl. Instr. and Meth. **A317** (1992) 47.

[14] OPAL Collaboration, G. Abbiendi *et al.*, Phys. Lett. **B493** (2000) 249.

[15] M. Skrzypek *et al.*, Comp. Phys. Comm. **94** (1996) 216;
M. Skrzypek *et al.*, Phys. Lett. **B372** (1996) 289.

[16] M.W. Grünewald and G. Passarino *et al.*, *Four-Fermion Production in Electron-Positron Collisions*, `hep-ph/0005309` (2000).

[17] ALEPH, DELPHI, L3, OPAL Collaborations and the LEP Electroweak Working Group and the SLD Heavy Flavour and Electroweak Groups, *A Combination of Preliminary Electroweak Measurements and Constraints on the Standard Model*, CERN-EP/2000-016 (2000), and references therein.

[18] E. Norrbin and T. Sjöstrand, *QCD Radiation off Heavy Particles*, `hep-ph/0010012` (2000).

[19] OPAL Collaboration, G. Abbiendi *et al.*, *Measurement of the Mass and Width of the W Boson in* e^+e^- *Collisions at 189 GeV*, CERN-EP-2000-099, submitted to Phys. Lett. B.

[20] A. Stuart and J. K. Ord, *Kendall's Advanced Theory of Statistics*, Vol. 2, Ch. 23 5th Ed., Oxford University Press, New York, (1991).

[21] ALEPH, DELPHI, L3, OPAL Collaborations, and the LEP working group for Higgs boson searches, *Search for Higgs bosons: Preliminary combined results using LEP data collected at energies up to 202 GeV,* CERN-EP/2000-055 (2000)

[22] R.D. Cousins and V.L. Highland, Nucl. Instr. and Meth. **A320** (1992) 331.

[23] ALEPH, DELPHI, L3 and OPAL Collaborations, and the LEP Higgs Working Group, in preparation.

Channel	Cut	Data	Total bkg.	$q\bar{q}(\gamma)$	4-fermi.	Eff. [%] (signal events)	
						110 GeV	115 GeV
Four-jet	Presel.	3820	3609.9	760.8	2859.4	85.2	86.9
	$\mathcal{L}^{HZ}$	60	49.8±6.0	12.8	37.0	45.5 (9.04±0.41)	41.8 (2.24±0.10)
Missing-E	Presel.	354	334.5	57.0	277.5	56.1	49.5
	$\mathcal{L}^{HZ}$	68	69.7±8.6	10.6	59.1	50.0 (4.70±0.28)	43.9 (1.68±0.10)
Tau	Presel.	343	334.5	57.0	277.5	48.3	43.3
	Final $\mathcal{L}$	8	11.1±1.2	0.4	10.7	29.5 (0.98±0.05)	22.9 (0.25±0.01)
Electron	Presel.	429	378.6	171.0	207.6	72.7	71.3
	$\mathcal{L}^{HZ}$	6	8.5±1.3	0.3	8.2	52.9 (0.66±0.02)	48.7 (0.17±0.004)
Muon	Presel.	79	66.2	36.8	29.4	70.3	70.9
	$\mathcal{L}^{HZ}$	10	7.0±1.0	0.2	6.8	59.1 (0.80±0.02)	59.9 (0.23±0.006)

Table 1: *The number of events after preselection and after the final likelihood selection for the 192–209 GeV data and the expected background. The errors on the total background and the expected Higgs signal include all systematic errors. The last two columns show the detection efficiencies (and the numbers of expected signal events in parentheses) for a Higgs boson with m_{H}=110 GeV and 115 GeV. For the four-jet channel, the efficiency is computed only for $\mathrm{H}^0 \to \mathrm{b\bar{b}}$ decays, and for the tau channel for the processes $\mathrm{H}^0\mathrm{Z}^0 \to \tau^+\tau^-(\mathrm{H}^0 \to$ all) or $\mathrm{H}^0\mathrm{Z}^0 \to \mathrm{q\bar{q}}\tau^+\tau^-$ assuming Standard Model branching fractions. For other channels, the efficiency is for all decays of the Standard Model Higgs boson.*

Candidates							
Candidate	Channel	$m_{\mathrm{H}}^{\mathrm{rec}}$ (GeV)	$\mathcal{L}^{\mathrm{H}^0\mathrm{Z}^0}$	E_{CM} (GeV)	s/b for m_{H} (GeV)		
					105	110	115
# 1	Four-jet	110.7	0.995	206.6	0.64	2.09	0.70
# 2	Four-jet	112.6	0.999	205.4	0.28	1.18	0.49
# 3	Missing-Energy	104.0	0.999	205.4	4.55	0.96	0.28
# 4	Missing-Energy	112.1	0.853	206.4	0.15	0.44	0.23
# 5	Tau	105.3	0.993	205.3	4.00	0.46	0.05
# 6	Electron	124.7	0.873	205.4	0.20	0.17	0.16
# 7	Muon	102.2	0.999	205.4	3.02	0.38	0.04

Table 2: *The candidates with the largest weights for the 115 GeV Higgs hypothesis in each channel. The columns labeled $m_{\mathrm{H}}^{\mathrm{rec}}$ and $\mathcal{L}^{\mathrm{H}^0\mathrm{Z}^0}$ are the reconstructed Higgs mass and selection likelihood values, respectively. The next three columns give the signal to background ratio (s/b) using the discriminants which are used in the confidence level calculation. The s/b values for Higgs boson test masses of 105, 110 and 115 GeV are shown. For the four-jet and the missing-energy channels, all candidates with s/b larger than 0.20 for 115 GeV are listed. For the tau, electron and muon channels, the candidates with the largest s/b for the 115 GeV hypothesis are listed in the lower portion of the table.*

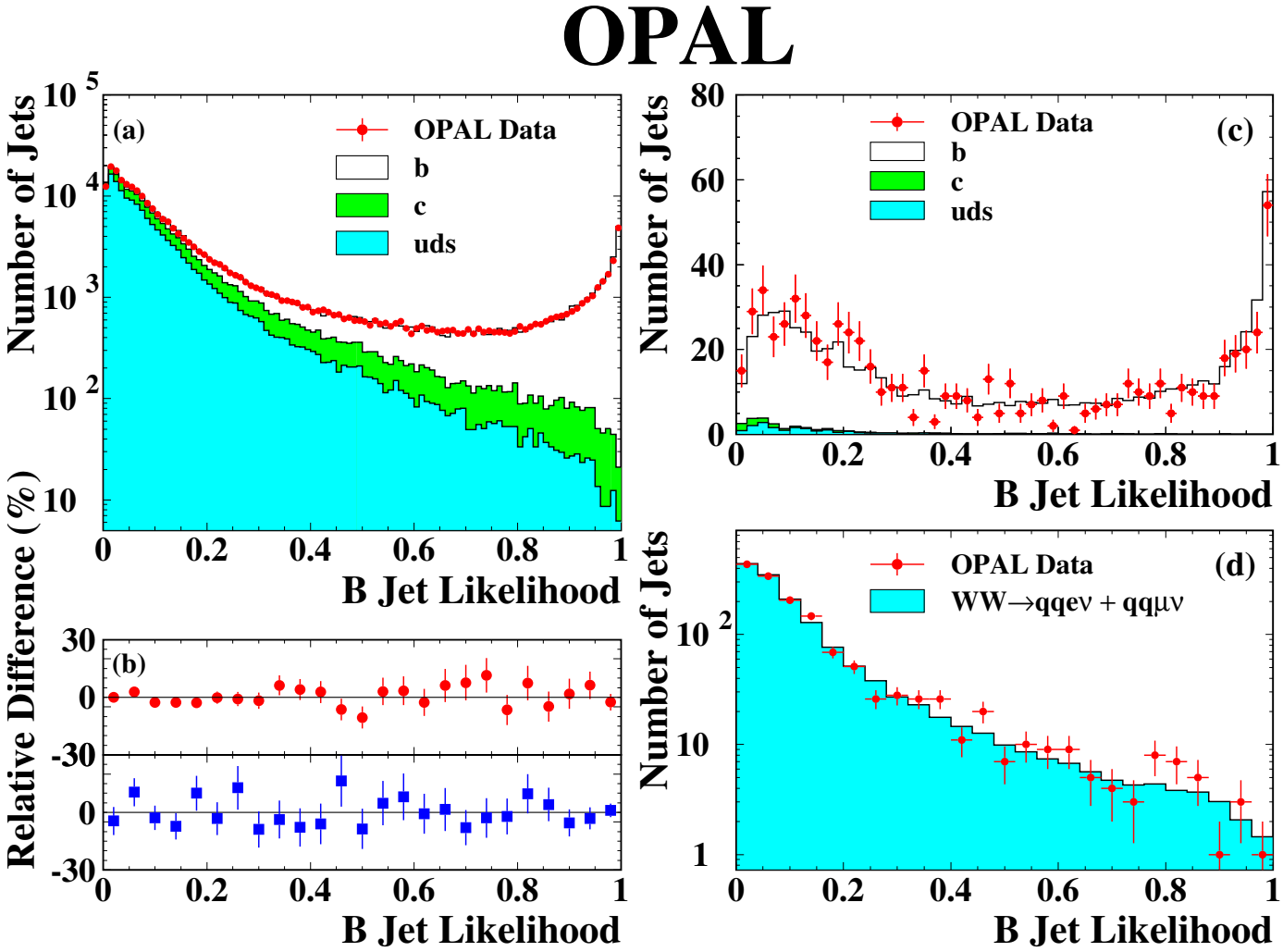

Figure 1: *The b-tagging performance and modelling for (a–b) calibration data taken at* $\sqrt{s} = m_{\mathrm{Z}}$ *in 2000, and (c–d) at* $\sqrt{s}$ *between 200–209 GeV in 2000. (a) The distribution of the b-tagging variable* $\mathcal{B}$ *for jets in data compared to the Monte Carlo expectation. (b) The bin-by-bin difference between data and Monte Carlo simulation for jets opposite non b-tagged jets (circles) and for jets opposite b-tagged jets (squares). (c) The b-tagging output,* $\mathcal{B}$*, for jets opposite b-tagged jets in a sample of* $\mathrm{q\bar{q}}\gamma$ *events, and (d) for jets in a sample of* $\mathrm{W^+W^-} \to \mathrm{q\overline{q}e^-\overline{\nu}_e}$ *and* $\mathrm{W^+W^-} \to \mathrm{q\overline{q}}\mu^-\overline{\nu}_\mu$ *events (and charge conjugates). The histogram in (d) shows the distribution from the four-fermion Monte Carlo samples.*

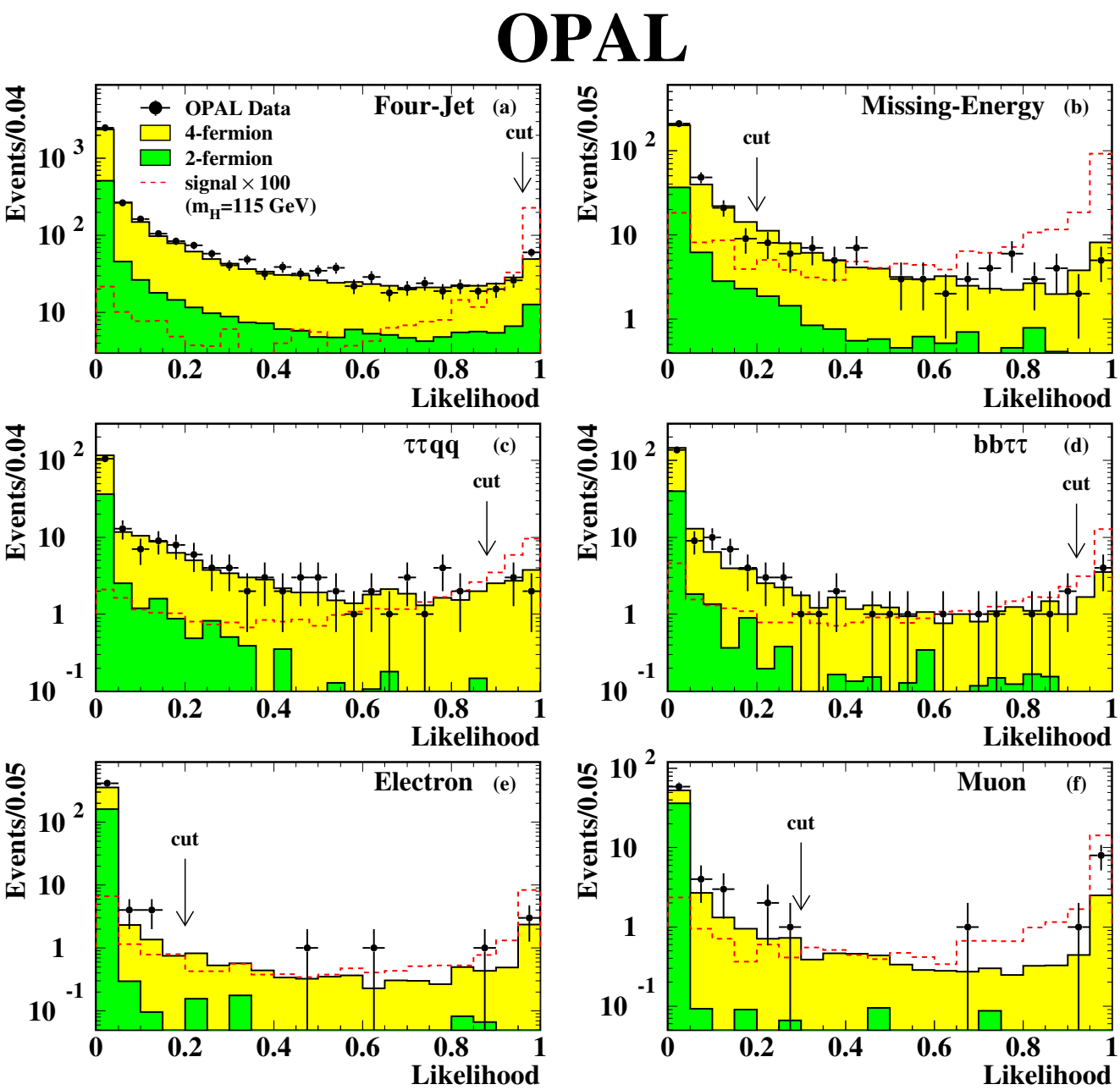

Figure 2: *The distributions of the likelihood output variables in* $\mathrm{H^0Z^0}$ *searches for the 1999 and 2000 data in: (a) the four-jet channel, (b) the missing-energy channel, (c) the tau channel* $\tau^+\tau^-\mathrm{q\bar{q}}$*, (d) the tau channel* $\mathrm{b\bar{b}}\tau^+\tau^-$*, (e) the electron channel and (f) the muon channel. OPAL data are shown with points, backgrounds with the shaded histograms, and the expectation from a signal with* m_{H}*=115 GeV with the dashed histograms (scaled up by a factor of 100 for visibility.)*

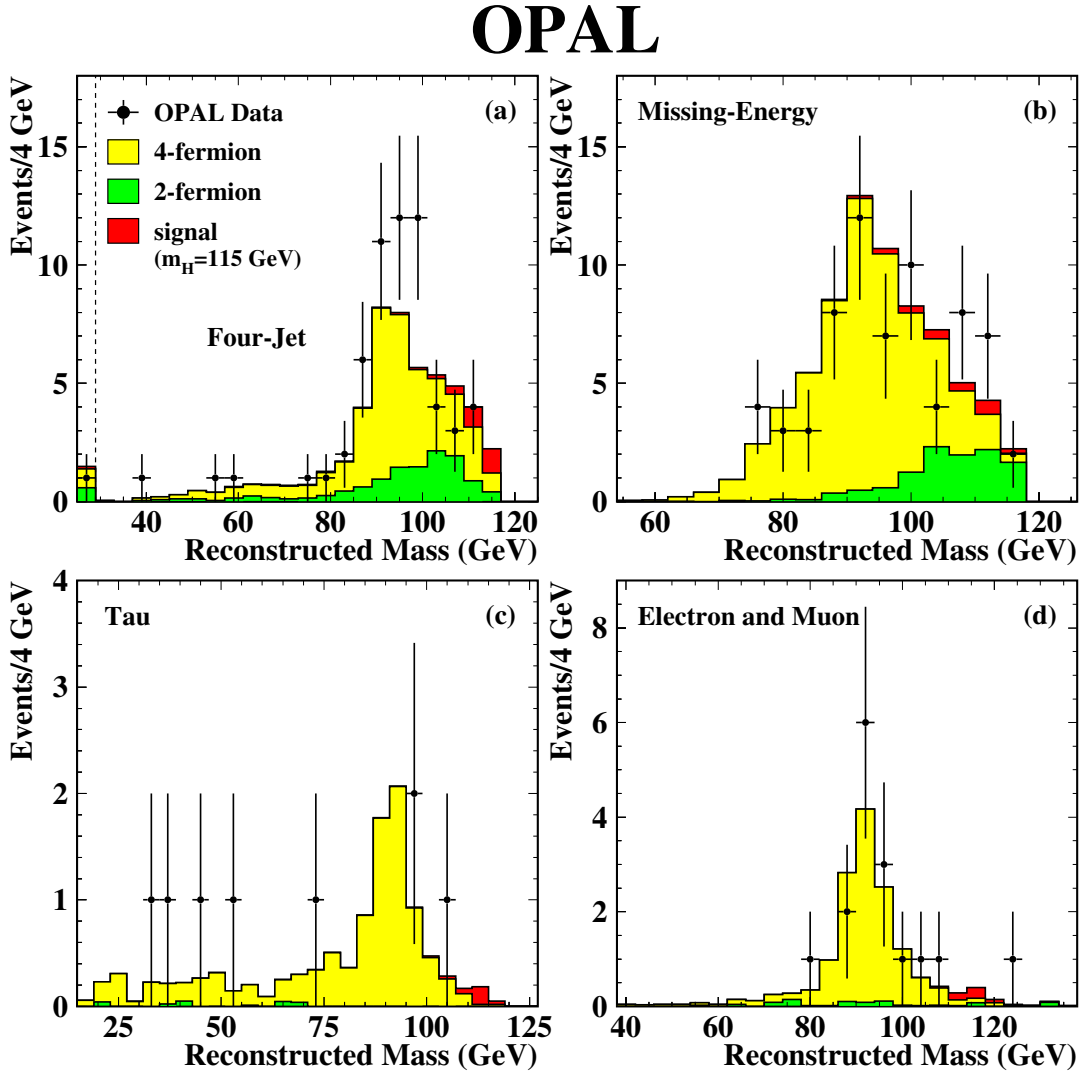

Figure 3: *The reconstructed mass distribution for the selected events in the 1999 and 2000 data for (a) the four-jet channel, (b) the missing-energy channel, (c) the tau channels, and (d) the electron and muon channels combined. The first bin in (a) contains all events with χ^2 probability of the H^0Z^0 5C kinematic fit $< 10^{-5}$ for chosen jet-pairings. The dark (light) grey area shows the expected contribution from the $q\bar{q}(\gamma)$ (four-fermion) process. The Standard Model signal expectation for 115 GeV is shown with the very dark histograms on top of the Standard Model backgrounds.*

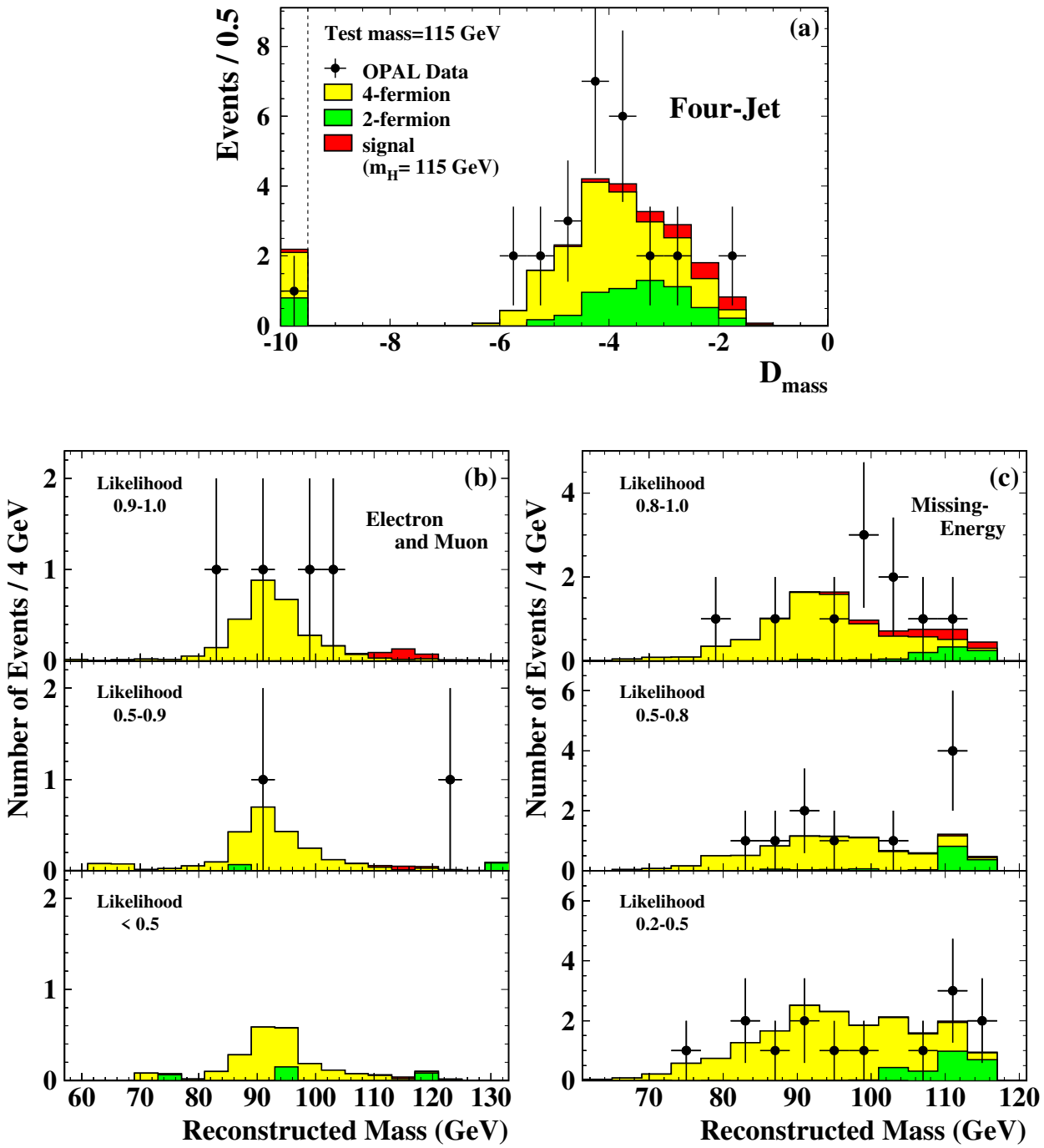

Figure 4: *(a) The distribution of the variable $\mathcal{D}_{mass}$ in the four-jet channel for a test mass of 115 GeV. (b) The reconstructed mass distribution in the electron and muon channels for the likelihood ranges of 0.9–1.0, 0.5–0.9, and range between the selection cut values (0.2 for the electron channel and 0.3 for the muon channel) and 0.5. (c) The reconstructed mass distribution in the missing-energy channel for the likelihood ranges of 0.8–1.0, 0.5–0.8, and 0.2–0.5. In all distributions, the data for $\sqrt{s} \geq 204$ GeV are shown with points, and the expected $q\bar{q}(\gamma)$ backgrounds are shown with dark-shaded histograms and the expected four-fermion backgrounds are shown with light-shaded histograms. The expected distributions from a 115 GeV Higgs boson signal are shown with very dark-shaded histograms.*

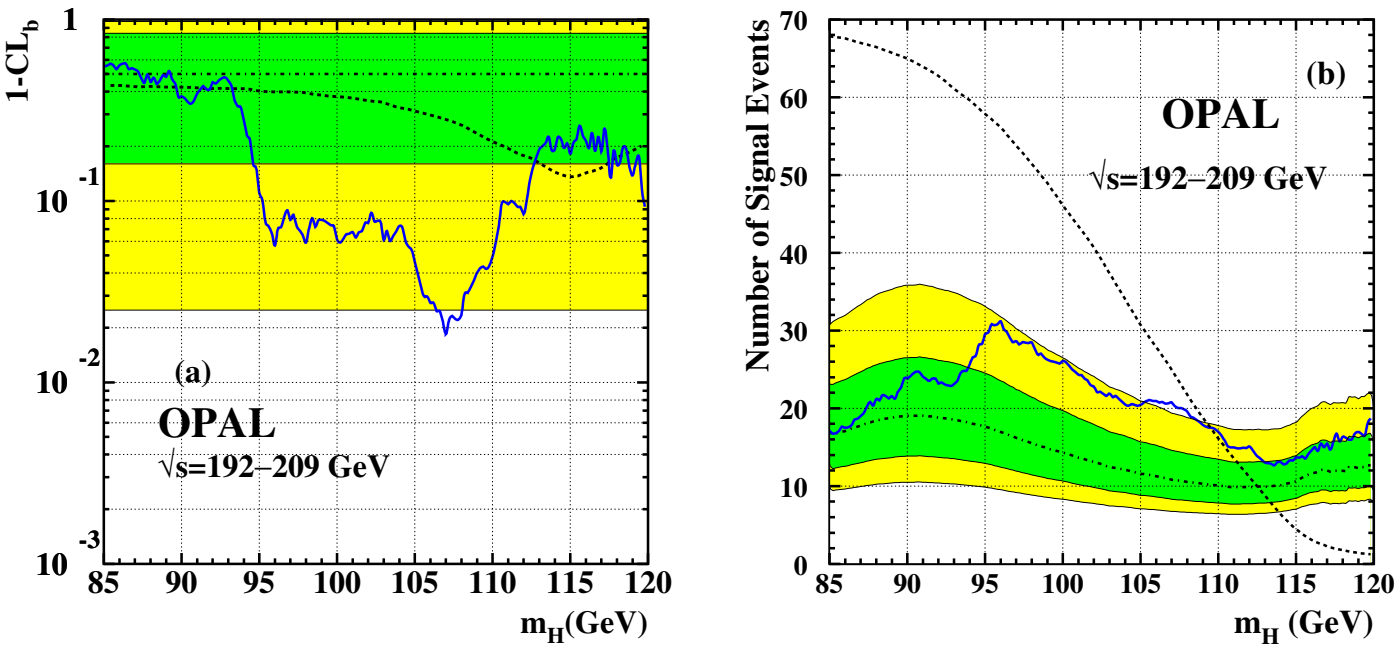

Figure 5: *(a) The confidence level for the background-only hypothesis,* $(1 - \mathrm{CL}_b)$*, as a function of the Higgs boson test mass. The dotted curve represents the median expectation assuming the presence of the Standard Model Higgs boson with a 115 GeV mass. The dark (light) shaded bands indicate the 68% (95%) probability intervals centred on 0.5, the median expectation in the absence of a signal, which is indicated with a dot-dashed line. (b) Upper limits on the signal counts at the 95% confidence level* (n_{95})*, as observed (solid line) and the expected median (dot-dashed line) for background-only experiments, as a function of the Higgs boson test mass. The expected rate of the accepted signal counts for a Standard Model Higgs boson with a mass equal to the test mass is shown with the dotted line. The shaded bands are the 68% and 95% probability intervals centred on the median background expectation. The range for the test mass* m_{H} *is chosen in both (a) and (b) to extend to 85 GeV to show the consistency of the 1999 and 2000 OPAL data with the background expectations near the* Z^0 *peak, even though previous OPAL search results [5] are sensitive to test masses below 100 GeV.*

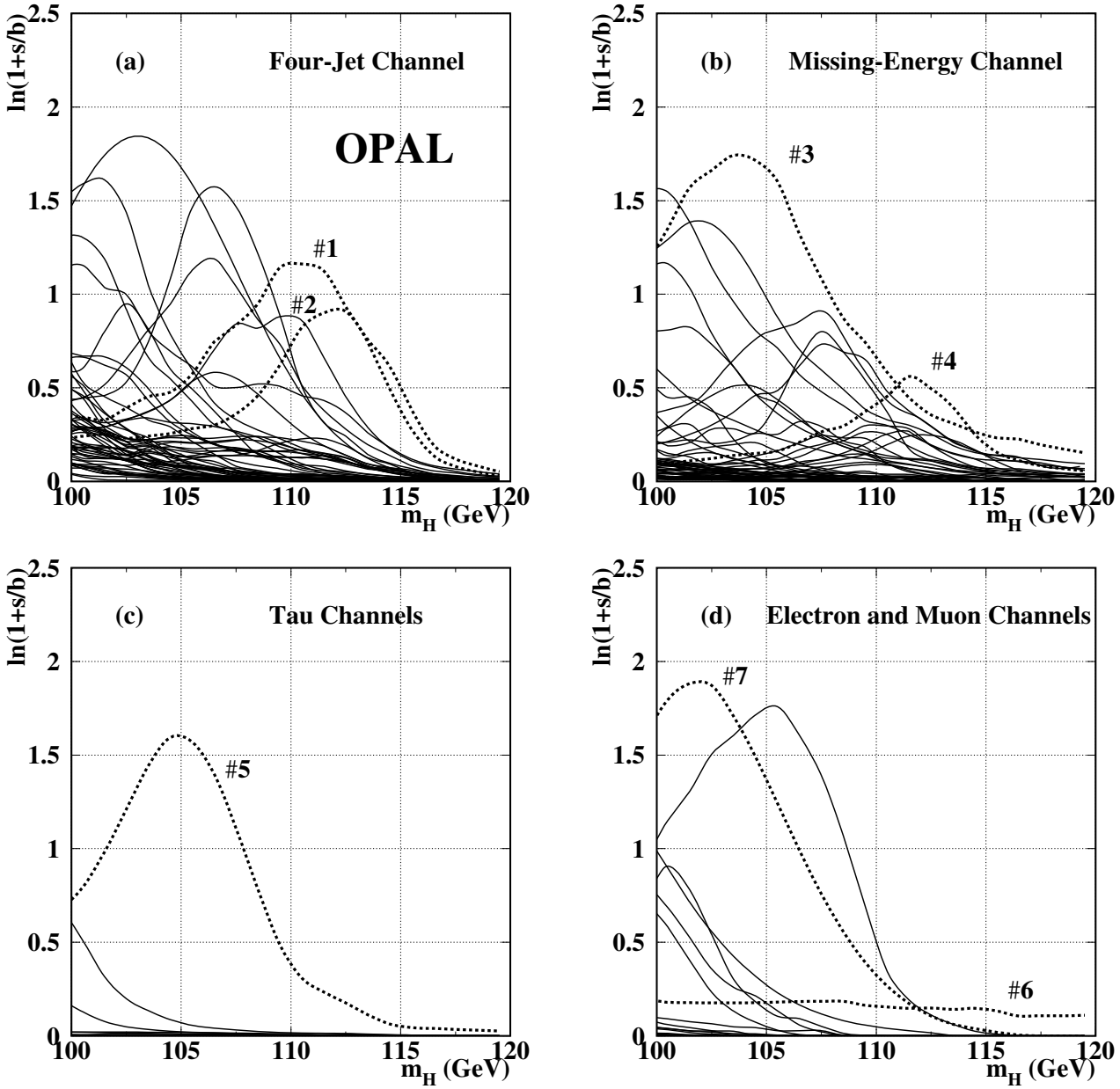

Figure 6: *The* $\ln(1+s/b)$ *distributions as a function of the Higgs boson test mass for each candidate collected in 1999 and 2000 for (a) the four-jet channel, (b) the missing-energy channel, (c) the tau channels, and (d) the electron and muon channels. Each curve in the plots represents the* $\ln(1+s/b)$ *of each candidate as a function of the Higgs boson test mass. The dotted lines show the contributions of the candidates listed in Table 2.*

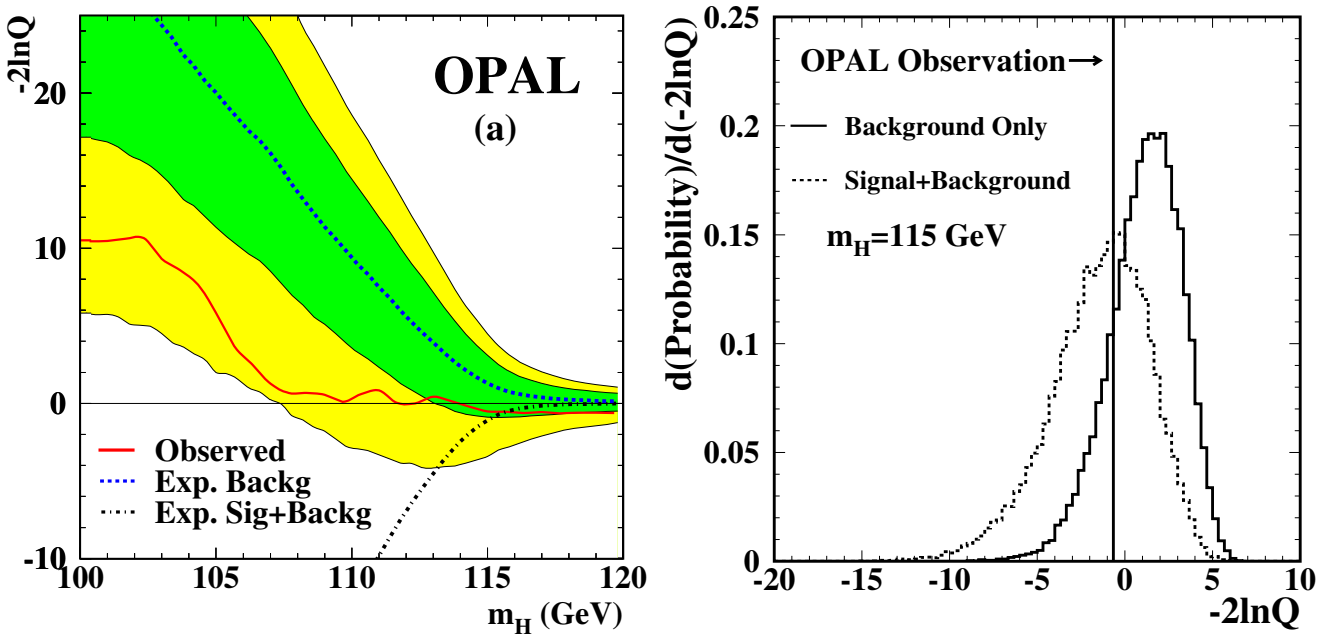

Figure 7: *(a) The log-likelihood ratio* $-2\ln Q$ *comparing the relative consistency of the data with the signal+background hypothesis and the background-only hypothesis, as a function of the test mass* m_{H}*. The observation for the data is shown with a solid line. The dashed line indicates the median background expectation and the dark (light) shaded band shows the 68% (95%) probability intervals centred on the median. The median expectation in the presence of a signal is shown with a dot-dashed line where the hypothesized signal mass is the test mass. (b) The* $-2\ln Q$ *distribution expected in a large number of fictitious background-only experiments (solid histogram), and in a large number of fictitious experiments in the presence of a 115 GeV Higgs boson (dashed histogram). The observation in the data is shown with a vertical solid line.*